C,N-chelated diaminocarbene platinum(II) complexes derived from 3,4-diaryl-1H-pyrrol-2,5-diimines and cis-dichlorobis(isonitrile)platinum(II)

Afanasenko, Anastasiia M.; Chulkova, Tatiana G.; Boyarskaya, Irina A.; Islamova, Regina M.; Legin, Anton A.; Keppler, Bernhard K.; Selivanov, Stanislav I.; Vereshchagin, Anatoly N.; Elinson, Michail N.; Haukka, Matti

Published in:
Journal of Organometallic Chemistry

DOI:
10.1016/j.jorganchem.2020.121435

Publication date:
2020

Journal of Organometallic Chemistry 923 (2020) 121435

Contents lists available at ScienceDirect

Journal of Organometallic Chemistry

journal homepage: www.elsevier.com/locate/jorganchem

C,N-chelated diaminocarbene platinum(II) complexes derived from 3,4-diaryl-1H-pyrrol-2,5-diimines and *cis*-dichlorobis(isonitrile) platinum(II): Synthesis, cytotoxicity, and catalytic activity in hydrosilylation reactions

Anastasiia M. Afanasenko [a], Tatiana G. Chulkova [b, *], Irina A. Boyarskaya [b], Regina M. Islamova [b], Anton A. Legin [c], Bernhard K. Keppler [c], Stanislav I. Selivanov [b], Anatoly N. Vereshchagin [d], Michail N. Elinson [d], Matti Haukka [e]

[a] Stratingh Institute for Chemistry, University of Groningen, Nijenborgh 4, 9747, AG Groningen, the Netherlands
[b] Saint Petersburg State University, Institute of Chemistry, 7/9 Universitetskaya Nab., Saint Petersburg, 199034, Russia
[c] Institute of Inorganic Chemistry, University of Vienna, Währinger Straße 42,1090, Vienna, Austria
[d] N. D. Zelinsky Institute of Organic Chemistry, 47 Leninsky Prospect, Moscow, 119991, Russia
[e] Department of Chemistry, University of Jyväskylä, P.O. Box 35, FI-40014, Jyväskylä, Finland

ARTICLE INFO

Article history:
Received 11 April 2020
Received in revised form
4 July 2020
Accepted 10 July 2020
Available online 24 July 2020

Keywords:
Anti-cancer activity
Catalysis
Diaminocarbene platinum(II) complexes
Hydrosilylation
Luminescence

ABSTRACT

The reaction of 3,4-diaryl-1*H*-pyrrol-2,5-diimines with *cis*-dichlorobis(isonitrile)platinum(II) affords the C,N-chelated diaminocarbene platinum(II) complexes, which have been fully characterized including molecular spectroscopy, single crystal X-ray diffraction and DFT calculations. The obtained platinum(II) complexes are effective catalysts for the hydrosilylation of alkynes and alkenes. Thus, the reaction of phenylacetylene with triethoxysilane leads to the formation of α- and β-(*E*)-vinylsilanes, generating TON's in the range of 10^3 to 10^4 and TOF's in the range of 10^2 to 10^3 h^{-1}. Also, the cross-linked silicones, possessing the luminescence properties, were obtained by the hydrosilylation reaction of vinyl- and hydride-containing polysiloxanes. Additionally, the efficiency of diaminocarbene platinum(II) complexes against CH1/PA-1, SW480, and A549 cancer cell lines has been demonstrated by *in vitro* cytotoxicity studies.

1. Introduction

In recent years, metal complexes bearing acyclic diaminocarbenes ([M]ADCs) [1,2] have emerged as a new family of homogeneous catalysts to be a prominent alternative to well-investigated metal-*N*-heterocyclic carbene ([M]NHCs) [3–5] species. Notwithstanding the structural and electronic similarity to the NHCs, the greater steric control due to the wider N–C–N bond angles of acyclic diaminocarbene ligands [6] as well as donor ability and the rotation freedom [7,8] ensure the high stability of the corresponding metal complexes and foster various stages of the catalytic processes [2].

Easy-to-prepare metal-ADCs complexes synthesized by nucleophilic addition of N-nucleophiles to coordinated isocyanides [9–11] have been successfully investigated as potential catalysts for several organic transformations (cross-coupling, metathesis, cyclization reactions, etc.) [12–15]. However, as far as it is known, examples of catalytic activities of the ADC-platinum(II) complexes for hydrosilylation of unsaturated compounds are quite limited to date. Recently, the first examples of the use of diaminocarbene platinum complexes derived from the reaction between *cis*-[$PtCl_2$(CN-R)$_2$] and hydrozones [16] or 3-iminoisoindolin-1-ones [17] as catalysts for hydrosilylation of unsaturated compounds have been reported.

In this context, as a continuation of these studies on the application of platinum systems as homogeneous catalysts for the hydrosilylation of unsaturated organic molecules, herein we have presented on the synthesis, characterization, *in vitro* antitumor activity studies, and reactivity of series of acyclic diaminocarbene complexes of Pt(II) for the hydrosilylation of both terminal alkynes and alkenes.

* Corresponding author.
E-mail address: t.chulkova@spbu.ru (T.G. Chulkova).

https://doi.org/10.1016/j.jorganchem.2020.121435
0022-328X/

2. Results and discussion

2.1. Synthesis and characterization of the ADC-platinum(II) complexes (3–5)

Compounds **3a**–**c**, **4c**, **5c** have been obtained in 20–50% yields by stirring for 2 h a mixture of 3,4-diaryl-1*H*-pyrrol-2,5-diimine (aryl = phenyl (**1a**), 4-methylphenyl (**1b**), 4-methoxypheyl (**1c**)) and *cis*-[$PtCl_2(CNR^2)_2$] (R^2 = cyclohexyl (**2a**), *tert*-butyl (**2b**), 4-methoxypheyl (**2c**)) in chloroform at room temperature (Scheme 1). 3,4-Diaryl-1*H*-pyrrol-2,5-diimines, containing electron-withdrawing substituents (aryl = 4-fluorophenyl (**1d**), 4-chlorophenyl (**1e**), 4-bromophenyl (**1f**)), react more slowly than the compounds with electron donor groups. Thus, employing 3,4-diaryl-1*H*-pyrrol-2,5-diimines (**1d**–**f**) as coupling partners, the reactions proceeded under reflux conditions for 5 h with the formation of the corresponding platinum complexes with yields of 12–22% (**3d**–**f**). Interestingly, the obtained products have the same structure as the ADC-palladium(II) complexes derived from 3,4-diaryl-1*H*-pyrrol-2,5-diimines and bisisocyanide palladium(II) complexes [18]. During the reaction, one isocyanide ligand in **2a**–**c** undergoes a nucleophilic attack by the imino group of **1a**–**f**, whereas the second one remains intact. The imino nitrogen atom of **1** is attached to the carbon atom of the isocyanide group, whereas the nitrogen atom of the pyrrole ring coordinates to the metal center, thus closing the five-membered metallocycle. As a result, monocarbene platinum(II) complexes were obtained.

The obtained diaminocarbene complexes **3**–**5** were fully characterized by elemental analysis, ESI^+-MS, IR, 1D and 2D NMR spectroscopies. The NMR spectral assignment to **3a**–**f**, **4c**, **5c** was performed on the basis of signal intensities, chemical shifts and $^1H,^1H$-coupling constants as well as the results of two-dimensional NMR measurements (COSY, NOESY, $^1H,^{13}C$-chemical shift correlation spectra (HSQC and HMBC)). For example, the correlations found in the COSY, $^1H,^{13}C$-HMBC, and $^1H,^{13}C$-HSQC spectra of **3b** correspond with the proposed structure (Fig. 1). In the $^1H,^{13}C$-HMBC spectrum (Fig. S9) of **3b**, the observed cross-peak between signals of H^{25b} (δ 9.93 ppm) and C^{17} (δ 140.9 ppm) allows to identify signals of aromatic ring **B**. The correctness of signal C^{17} assignment is additionally confirmed by the presence of cross-peak between H^{19}, H^{24} (δ 7.36 ppm) and C^{17} (δ 140.9 ppm). In the COSY spectrum (Fig. S10), the cross-peaks between H^2 (δ 4.53 ppm) and the nearest protons H^3, H^7 (δ 2.23–2.26 ppm/1.89–1.92 ppm), having the axial and equatorial orientations, respectively, are observed. Thus, the presence of these cross-peaks assists the identification of cyclohexyl ring **C**. Similar cross-peaks between H^{27} (δ 3.57 ppm) and axial/equatorial protons H^{28}, H^{32} (δ 1.55–1.63 ppm/1.83–1.87 ppm, respectively) define the cyclohexyl ring **D**.

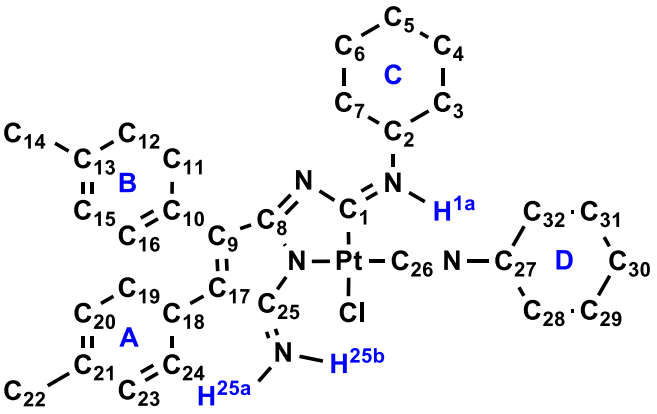

Fig. 1. Structure of **3b**.

In the fragment **B** of NOESY spectrum (Fig. S12), the cross-peak between H^{11}, H^{16} (δ 7.45 ppm) and equatorial protons H^3, H^7 and H^4, H^6 (δ 1.89–1.92 ppm/1.83–1.87 ppm, respectively) is observed. The presence of these spatial interactions does not contradict the data of X-ray analysis about the mutual spatial arrangement of the rings **B** and **C**. In the fragment **A** of NOESY spectrum (Fig. S12), a direct interaction between H^{25b} (δ 9.93 ppm) and equatorial protons H^{29}, H^{31} (δ 1.55–1.63 ppm) of cyclohexyl ring **D** is observed; the existence of this spatial interaction proves the existence of **3b** dimers in a chloroform solution. In the fragment **B** of NOESY spectrum (Fig. S12), the cross-peak between signals of aromatic ring protons H^{19}, H^{24} (δ 7.36 ppm) and equatorial protons of cyclohexyl fragment H^{29}, H^{31} (δ 1.55–1.63 ppm) is identified. These aforementioned direct interactions additionally prove the correctness of signal assignment in the aromatic and aliphatic fragments.

The structure of **3b** was additionally confirmed by single crystal X-ray diffraction (Fig. 2, Table S2).

The crystals of **3b** suitable for X-ray diffraction were obtained by a slow evaporation of dichloromethane at room temperature. **3b** is crystallized in the monoclinic space group *C2/c*. The Pt center has distorted square planar geometry. The cyclohexyl isocyanide ligand is located opposite to the pyrrole ring. Earlier in our group, similar ADC-platinum(II) complexes have been obtained via coupling between 3-iminoisoindolin-1-one and bisisocyanide platinum(II) species, however, the geometry of these complexes is different: the isocyanide ligand is located opposite to the diaminocarbene fragment [19].

We assume whether one or another isomer is obtained probably depends on the stabilization of the compound due to the formation of hydrogen bonds. In the case of platinum(II) complex with

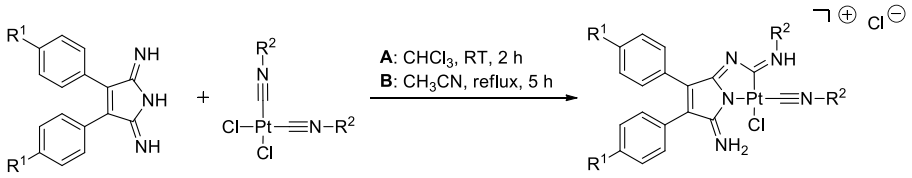

1a: R^1 = H
1b: R^1 = CH_3
1c: R^1 = CH_3O
1d: R^1 = F
1e: R^1 = Cl
1f: R^1 = Br

2a: R^2 = Cy
2b: R^2 = *t*-Bu
2c: R^2 = 4-$CH_3OC_6H_4$

3: R^2 = Cy; R^1 = H (**a**), CH_3 (**b**), CH_3O (**c**), F (**d**), Cl (**e**), Br (**f**)
4: R^2 = t-Bu; R^1 = CH_3O (**c**)
5: R^2 = 4-$CH_3OC_6H_4$; R^1 = CH_3O (**c**)

Scheme 1. Syntheses of ADC-platinum(II) complexes (**3a**–**f**, **4c**, **5c**).

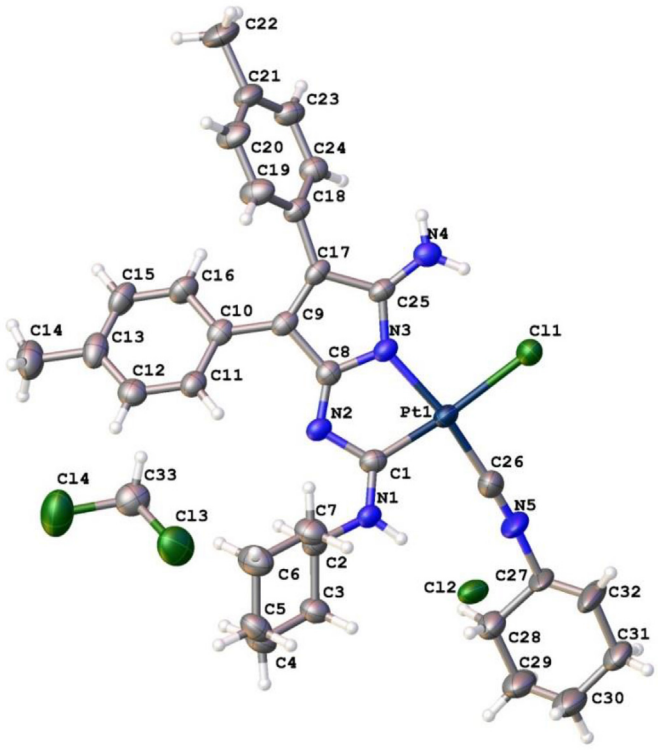

Fig. 2. Molecular structure of **3b**·CH_2Cl_2 at the 50% probability level.

iminoisoindolinone fragment, the product is stabilized via the NH···Cl hydrogen bond, whereas, the structure of **3b** is stabilized by two hydrogen bonds ((N4)H···Cl1 (2.32(7) Å) and (N1)H···Cl2 (2.28(7) Å)). Indeed, according to our theoretical calculations, the obtained isomer of **3b** (Fig. 2) is 22.3 kJ/mol more stable than its other isomer **3b'**. The optimized geometry of **3b** is close to the structure obtained by XRD. Also, the (NH)H···Cl(Pt) (2.308 Å) and (NCy)H···Cl(Pt) (2.433 Å) intramolecular hydrogen bond lengths were calculated for **3b** and **3b′**, respectively. These data show that the (NH)H···Cl(Pt) intramolecular hydrogen bond in **3b** is stronger than the (NCy)H···Cl(Pt) bond in its isomer **3b'**.

2.2. Photophysical properties

The absorption and fluorescence properties of the synthesized compounds **3a**–**d**, **4c**, and **5c** were evaluated by UV–vis absorption and emission spectroscopies at a concentration of $2.5 \cdot 10^{-5}$ M in chloroform (Table 1). Compounds **3a**–**d**, **4c**, and **5c** show the maximum absorbance at larger wavelengths (λ_{abs} at 318–398 nm) (Table 1, Fig. S13) compared to those of **1a**–**d** (λ_{abs} at 278–311 nm) [20]. The red-shift of the absorption maximum band can be explained by the formation of an extended π-conjugated system in the resulting metal complex structure. The presence of the donor substituents at the phenyl rings of the 1*H*-pyrrol-2,5-diimine fragment leads to the red-shift of the absorption band like in **1a**–**d**.

Complexes **3a**–**d**, **4c**, and **5c** exhibit fluorescence in the visible range of 493–572 nm (Table 1, Figs. S14–15). As in the case of the absorption spectra, donor substituents at the phenyl rings of the pyrroldiimine fragment generally cause red shift of the fluorescence emission bands. The fluorescence spectra of **3a**–**d**, **4c**, and **5c** have large Stokes shifts varied in the range of 174–185 nm. The measured fluorescence lifetimes for **3a**–**d**, **4c**, and **5c** are in the range of 10–13 ns (Table S1). Similarly to the previously reported Pd analogues [18], all investigated diaminocarbene platinum complexes possess low luminescence (the fluorescence quantum yields for **3a**–**d**, **4c**, and **5c** vary in a range of 1–11% (Table S1)).

Table 1
Absorption and emission properties of **3a**–**d**, **4c**, and **5c** in chloroform solution ($2.5 \cdot 10^{-5}$ M).

Compound	λ_{abs}, nm ($\varepsilon \cdot 10^{-4}$, $M^{-1}cm^{-1}$)	λ_{em}, nm	Stokes shift, nm
3a	318 (1.1)	493	175
3b	268[a], 329 (0.9)	505	176
3c	268[a], 390 (1.2)	571	181
3d	353 (1.0)	530	177
4c	268[a], 398 (0.6)	572	174
5c	270[a], 382 (0.7)	567	185

[a] The band appears as a shoulder, the position of the maximum is approximately determined.

2.3. In vitro cytotoxic activity

To date, a large number of studies on the cytotoxicity of NHC complexes with various metals have been carried out [21,22]. Despite extensive studies on ADC complexes in organometallic chemistry and catalysis, only a restricted array of anticancer applications have been reported so far for platinum, palladium, and gold derivatives [23–25]. To assess the anticancer potential of the obtained acyclic diaminocarbene platinum(II) complexes (**3b**, **4c**, and **5c**) their cytotoxic properties have been evaluated *in vitro* on ovarian teratocarcinoma (CH1/PA-1), colon carcinoma (SW480) cell lines and adenocarcinomic human alveolar basal epithelial cells (A549) (Fig. S18). The inhibitory potency of the metal complexes on proliferation and viability of these cancer cells was characterized by using the spectrophotometric MTT assay, the obtained data is summarized in Table 2.

Cytotoxicity of all complexes is in a low to average micromolar range. The complexes were shown to effectively decrease the number of treated cancer cells. However, their efficiency is lower than shown for established cytotoxic anticancer drug cisplatin in respective cell lines.

2.4. ADC-Pt(II) catalysed hydrosilylation of phenylacetylene with triethoxysilane

^{1}H NMR studies of the reaction of phenylacetylene with triethoxysilane at 100 °C in the presence of catalytic amounts of the ADC-Pt(II) complexes evidenced that the studied catalysts promote the hydrosilylation of phenylacetylene to (*E*)-triethoxy(styryl) silane (β-(*E*)-product) as a major product and triethoxy(1-phenylvinyl)silane (α-product) as a minor product (Scheme 2). The formation of (*Z*)-triethoxy(styryl)silane (β-(*Z*)-isomer) was not observed.

In preliminary optimization of the reaction conditions, we revealed the influence of reaction time on the yield and product ratio (Table 3).

While no alkenes were obtained for 0.5 h (Table 3, entry 1), which could be attributed to the induction period of the catalyst [27], relatively good conversion of 61% for 1 h (Table 3, entry 2) and excellent - 87% for 3 h (Table 3, entry 5) were detected. Selecting

Table 2
In vitro cytotoxic activity of platinum complexes in CH1/PA-1, SW480, and A549 cell lines (IC_{50}, μM, 96 h exposure).

	3b	4c	5c	Cisplatin [26]
CH1/PA-1	13 ± 0.2	47 ± 2	15 ± 3	0.14 ± 0.03
SW480	12 ± 1	37 ± 7	13 ± 2	3.3 ± 0.4
A549	26 ± 1	>80	33 ± 2	1.3 ± 0.4

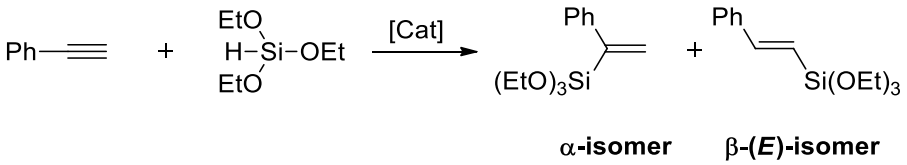

Scheme 2. Hydrosilylation of phenylacetylene.

Table 3
Optimization of the reaction conditions: effect of the reaction time.[a,b].

Entry	Time, h	Overall yield, %	α/β-(*E*) product ratio, %	TON	TOF, h^{-1}
1	0.5	0	–	–	–
2	1	61	21/79	12.2×10^2	4.1×10^2
3	2	73	23/77	14.6×10^2	4.9×10^2
4	2.5	80	26/74	16.0×10^2	5.3×10^2
5	3	87	27/73	17.4×10^2	5.8×10^2

[a] PhC≡CH (0.5 mmol, 1 equiv.), $(EtO)_3SiH$ (0.5 mmol, 1 equiv.), catalyst **3c** (5×10^{-2} mol%), toluene (0.2 mL). [b] Yields were determined by ^1H NMR spectroscopy using 1,2-dimethoxyethane as a standard; the isomeric content was determined on the basis of the alkene coupling constants (see the Supporting Information, p. S14).

appropriate reaction time (3 h), solvent (toluene) and reaction temperature (100 °C) for further study, the effect of catalyst loading was evaluated (Table 4). Notably, with 0.1 mol% and 0.05 mol% loading of catalyst, excellent yields of the corresponding alkenes were observed (93% and 87%, respectively). Importantly, the maximum catalyst turnover number (TON) of 7.8×10^3 was achieved with 0.005 mol% loading of catalyst **3c** during 3 h at 100 °C (Table 4, entry 3), however, the yield of the desired alkene products was dropped to 39%.

With the optimized reaction conditions at hand, the comparison of the catalytic activity of the acyclic diaminocarbene platinum(II) complexes **3a**–**d**, **4c**, **5c** as a function of the substituents in diaminocarbene (Table 5) and *1H*-pyrrol-2,5-diimine (Table 6) moieties was estimated in the model system. To our delight, all acyclic diaminocarbene complexes of Pt(II) could be potentially used as catalysts for the hydrosilylation reaction of terminal alkynes. Among the examined complexes, the most active species (**3b**, **3c**, **4c**, **5c**) were derived from the addition of 3,4-diaryl-*1H*-pyrrol-2,5-diimines with donor substituents ($R^1 = CH_3O$, CH_3) to isocyanide complexes of platinum(II), with bulky donor ligands ($R^2 =$ *t*-Bu, Cy, *p*-$(CH_3O)C_6H_4$), whereas **3a** and **3d** possess lower activity. The observed phenomenon could be attributed to the strong electron donation from the aminocarbenes, derived from the aliphatic isocyanides and *1H*-pyrrol-2,5-diimines, comprising donor substituents, to the metal center, facilitating the oxidative addition of silane substrates. The nature of the substituent R^2 has practically no effect on the yield of reaction products.

Notably, the isomeric ratio of alkene products is essentially independent of the nature of the substituents in the catalyst, namely, α- and β-(*E*)-products were observed in 1: 3 ratio.

2.5. ADC-Pt(II) catalysed curing of polysiloxanes

ADC-Pt(II) catalysed hydrosilylative cross-linking was studied on model α,ω-di(vinyldimethylsiloxy)poly(dimethylsiloxane) (PDMS)/trimethylsilyl-terminated poly(dimethylsiloxane-co-ethylhydrosiloxane) (EHDMS) mixtures with catalysts **3b**, **3d**, and **5c** (10^{-3}–$5 \cdot 10^{-5}$ M) (Scheme 3).

The catalytic activity was evaluated at 85 °C owing to the identification of the curing time (τ_{curing}) (Table S3).

Investigating the dependence of curing time (τ_{curing}) on the concentration of the platinum catalysts, we observed the gradual decline of the reaction time with increasing catalyst concentration, for instance, for the curing using **3b** at 5×10^{-5} M takes 15 h (Table S3, entry 4) vs 8 h at 1×10^{-3} M (Table S3, entry 1). Remarkably, we observed a clear correlation between the catalytic activity of the studied complexes and their structure. Catalyst 5c exhibits the highest catalytic activity, which is probably due to the presence of electron-donating methoxy-groups in its structure. Since it is known that the increasing donor character of a ligand increases the electron density at the metal center and favors the oxidative addition stage of the catalytic cycle. In contrast, complex **3d** demonstrates lower catalytic activity due to the large –I-effect of fluorine.

The obtained silicone formulations incorporate no structural defects, i.e. no bubbles and the surface of the silicone rubbers is uniform.

Further, we evaluated the luminescence properties of the silicone rubbers prepared employing catalysts **3a**–**d** and **5c** (Table 7).

It is worth noting that the emission maxima for the silicone rubbers obtained using catalysts **3a**–**d** and **5c** (Table 7 and Fig. S16) are blueshifted compared with chloroform solutions of complexes **3a**–**d** and **5c** (Table 1), respectively. The overall emission intensity for the cured silicone rubbers has substantially decreased when compared to that of complexes **3a**–**d** and **5c** in solution. The quantum yield cannot be carefully estimated for rubbers because of the complexity of calculations and polymer self-absorption.

Table 4
Optimization of the reaction conditions: effect of the catalyst loading.[a,b].

Entry	Catalyst 3c loading, mol%	Time, h	Overall yield, %	α/β-(*E*) product ratio, %	TON	TOF, h^{-1}
1	0.1	3	93	22/78	9.3×10^2	3.1×10^2
2	5×10^{-2}	3	87	27/73	17.4×10^2	5.8×10^2
3	5×10^{-3}	3	39	17/83	7.8×10^3	2.6×10^3

[a] PhC≡CH (0.5 mmol, 1 equiv.), $(EtO)_3SiH$ (0.5 mmol, 1 equiv.), toluene (0.2 mL). [b] Yields were determined by ^1H NMR spectroscopy using 1,2-dimethoxyethane as a standard; the isomeric content was determined on the basis of the alkene coupling constants.

Table 5
Effect of the substituents in diaminocarbene fragment.[a,b].

Entry	Catalyst	Overall yield, %	α/β-(*E*) product ratio, %	TON	TOF, h^{-1}
1	**3c**	87	27/73	17.4×10^2	5.8×10^2
2	**4c**	87	27/73	17.4×10^2	5.8×10^2
3	**5c**	81	20/80	16.2×10^2	5.4×10^2

[a] PhC≡CH (0.5 mmol, 1 equiv.), $(EtO)_3SiH$ (0.5 mmol, 1 equiv.), catalyst 3c, 4c, 5c (5×10^{-2} mol%), toluene (0.2 mL). [b] Yields were determined by ^1H NMR spectroscopy using 1,2-dimethoxyethane as standard; the isomeric content was determined on the basis of the alkene coupling constants.

Table 6
Effect of the substituents in *1H*-pyrrol-2,5-diimine fragment.[a,b].

Entry	Catalyst	Overall yield, %	α/β-(*E*) product ratio, %	TON	TOF, h^{-1}
1	**3a**	79	23/77	15.8×10^2	5.3×10^2
2	**3b**	90	21/79	18.0×10^2	6.0×10^2
3	**3c**	87	27/73	17.4×10^2	5.8×10^2
4	**3d**	74	23/77	14.8×10^2	4.9×10^2

[a] PhC≡CH (0.5 mmol, 1 equiv.), $(EtO)_3SiH$ (0.5 mmol, 1 equiv.), catalyst 3a−d (5×10^{-2} mol%), toluene (0.2 mL). [b] Yields were determined by ^1H NMR spectroscopy using 1,2-dimethoxyethane as standard; the isomeric content was determined on the basis of the alkene coupling constants.

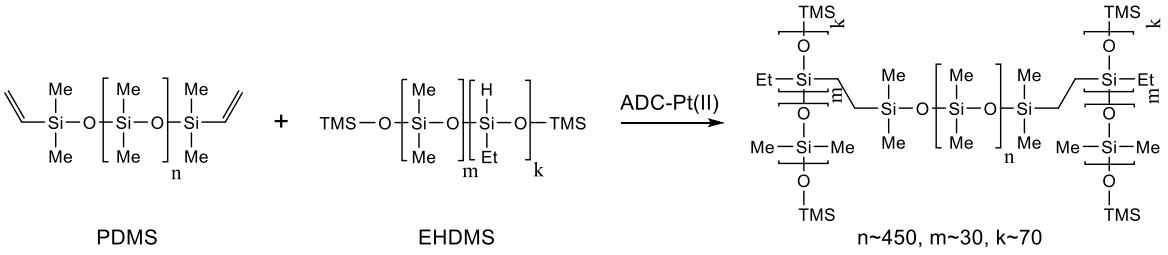

Scheme 3. ADC-Pt(II) catalysed cross-linking of PDMS and EHDMS.

Table 7
Luminescence properties of the silicone rubbers prepared using catalysts **3a**−**d** and **5c**.

Catalyst	λ_{ex}, nm	λ_{em}, nm	Stokes shift, nm
3a	353	477	124
3b	377	463	86
3c	375	526	151
3d	369	488	119
5c	384	507	123

3. Conclusion

In conclusion, we have successfully synthesized new ADC-Pt(II) complexes *via* the reaction of bisisocyanide platinum(II) complexes and 3,4-diaryl-*1H*-pyrrol-2,5-diimines and applied them as catalysts for the hydrosilylation of phenylacetylene. Employing optimized reaction conditions (toluene, 100 °C, 3 h, 0.05 mol% catalyst loading), the target vinylsilanes were obtained in good to excellent yields. It is crucial to mention that a limited number of the previously described hydrosilylation reactions catalysed by the Pt-(NHC) [27−30] and Pt-(ADC) [16,17] complexes require a higher catalyst loading (0.1−1 mol%) or a longer reaction time (up to 48 h). Also, the prepared ADC-Pt(II) complexes can be used as catalysts for the cross-linking of polysiloxanes leading to luminescent silicone rubbers.

Furthermore, we have revealed that the designed diaminocarbene platinum(II) complexes exhibit photoluminescent properties strongly depending on the substituents in pyrroldiimine moiety and demonstrate the promising potential as anticancer drugs.

4. Experimental

4.1. General considerations

All solvents were dried and purified by conventional methods and were freshly distilled under argon shortly before use. Other reagents were used without further purification. The starting materials 3,4-diaryl-1*H*-pyrrol-2,5-diimine (aryl = phenyl (**1a**), 4-methylphenyl (**1b**), 4-methoxypheyl (**1c**), 4-fluorophenyl (**1d**), 4-chlorophenyl (**1e**), 4-bromophenyl (**1f**)) [20,31,32] and *cis*-$[PtCl_2(CNR^2)_2]$ (R^2 = Cy (**2a**), *t*-Bu (**2b**), 4-$(CH_3O)C_6H_4$ (**2c**)) [33,34] were prepared as previously reported.

PDMS (the weight average molecular weight M_w = 80,000, the number average molecular weight M_n = 33,800, 0.5 wt% of CH=CH_2) and EHDMS (M_w = 8150, M_n = 4600, M_w/M_n = 1.8, Si−H 0.7 wt%) were obtained according to the procedure [35].

FTIR spectra were recorded on Shimadzu FTIR-8400S (4000−400 cm^{-1}) and IRAffinity-1S (4000−300 cm^{-1}) spectrometers using KBr pellets. One-dimensional (^1H, $^{13}C\{^1H\}$) and two-dimensional ($^1H-^{13}C$ HMBC, $^1H-^{13}C$ HSQC, NOESY, COSY) NMR spectra were recorded on a Bruker-DPX 400 instrument at ambient temperature. Electrospray ionization mass spectra were obtained on a Bruker micrOTOF spectrometer equipped with electrospray ionization (ESI) source using MeOH as the solvent. The instrument was operated in both positive and negative ion modes using a *m*/*z* range of 50−3000. The capillary voltage of the ion source was set at −4500 V (ESI^+−MS) and the capillary exit at ±(70−150) V. The nebulizer gas flow was 0.4 bar and drying gas flow 4.0 L/min. Elemental analyses were measured on a Euro EA3028-HT Element Analyzer system. The absorption spectra were recorded on a Perkin−Elmer precision spectrophotometer Lambda 1050. The

emission spectra, excitation spectra, and measurements of the lifetimes of excited states were measured on a modular spectrofluorimeter Fluorolog-3 (Horiba Jobin Yvon). Fluorescence lifetime measurements are based on time-correlated single photon counting (TCSPC). Device also includes an integrating sphere Quanta-ϕ with fiber optics which enables direct measurement of quantum yields of luminescence.

4.2. Synthesis of Pt(II) complexes

Synthesis of complexes **3a**−**c**, **4c**, and **5c**: A 50 mL flat-bottomed flask, equipped with a stirring bar, was charged with 3,4-diaryl-1*H*-pyrrol-2,5-diimine (aryl = phenyl (**1a**), 4-methylphenyl (**1b**), 4-methoxypheyl (**1c**)) (0.1 mmol), *cis*-[$PtCl_2(CNR^2)_2$] (R^2 = Cy (**2a**), *t*-Bu (**2b**), 4-(CH_3O)C_6H_4 (**2c**)) (0.1 mmol), and 10 mL of anhydrous chloroform. The reaction mixture was stirred at room temperature for 2 h: the color of the reaction mixture was immediately changed to cherry-red. After removal of the solvent under vacuum, the residue was washed with 10 mL of acetone. The resulting solid was recrystallized from the mixture of dichloromethane and hexane (2:1) at room temperature.

3a: Yield 46%, orange crystals. ^{1}H NMR (400 MHz, DMSO-d_6/$CDCl_3$): δ 10.71 (br, 1H, NH), 9.74 (br, 1H, NH), 7.54−7.34 (m, 10H, H−Ar), 4.45−4.39 (m, 2H, CH), 1.94−1.12 (m, 20H, −HC(CH_2)$_5$). ^{13}C NMR (101 MHz, DMSO-d_6): δ 182.1, 174.2, 172.1, 140.3, 137.1, 137.0, 130.8, 130.5, 130.3, 130.2, 130.1, 129.7, 129.2, 128.9, 128.8, 128.6, 55.7, 54.9, 31.7, 31.4, 25.1, 24.9, 22.3. IR (KBr, selected bands, cm^{-1}): 3407 w ν(N−H), 2935 s, 2856 s ν(C_{sp3}-H), 2234 s ν(C≡N), 1687 m, 1618 m ν(C = N), 1559 s ν(N−$C_{carbene}$). HRMS (ESI^+), *m*/*z*: 695.2235 $[M-Cl]^+$. $C_{30}H_{35}ClN_5Pt$ Calcd. m/z: 695.2229. Anal. Calcd. for $C_{30}H_{35}Cl_2N_5Pt\cdot 2CHCl_3$ (970.37): C, 39.61; H, 3.84; N, 7.22. Found: C, 40.14; H, 3.90; N, 7.34.

3b: Yield 50%, orange crystals. ^{1}H NMR (400 MHz, $CDCl_3$): δ 11.22 (br, 1H, NCNH^{1a}), 9.93 (br, 1H, NH^{25b}), 8.34 (br, 1H, NH^{25a}), 7.45 (d, $^3J_{HH}$ = 8.0 Hz, 2H, H^{11}, H^{16}), 7.36 (d, $^3J_{HH}$ = 8.0 Hz, 2H, H^{19}, H^{24}), 7.29 (d, $^3J_{HH}$ = 8.0 Hz, 2H, H^{20}, H^{23}), 7.15 (d, $^3J_{HH}$ = 8.0 Hz, 2H, H^{12}, H^{15}), 4.53 (br, 1H, CH^2NC), 3.57 (br, 1H, CH^{27}NC), 2.43 (s, 3H, CH_3 in A ring), 2.39 (s, 3H, CH_3 in B ring), 2.26−2.23 (m, 2H, H^{ax} at C^3, C^7), 1.92−1.89 (m, 2H, H^{eq} at C^3, C^7), 1.87−1.83 (m, 4H, H^{eq} at C^{28}, C^{32}; H^{eq} at C^4, C^6), 1.65−1.58 (m, 6H, H^{ax} at C^{28}, C^{32}; H^{eq} at C^{29}, C^{31}; H^{ax}, H^{eq} at C^5), 1.31−1.23 (m, 6H, H^{ax} at C^4, C^6; H^{ax} at C^{29}, C^{31}; H^{ax}, H^{eq} at C^{30}). ^{13}C NMR (101 MHz, $CDCl_3$): δ 183.8 (C^1), 179.4 (C^8), 170.8 (C^{25}), 140.9 (C^{17}), 140.8 (C^{21}), 140.6 (C^{13}), 138.2 (C^9),130.3 (C^{20}, C^{23}), 130.1 (C^{11}, C^{16}), 129.7 (C^{19}, C^{24}), 129.2 (C^{12}, C^{15}), 126.5 (C^{10}), 125.1 (C^{18}), 58.3 (C^2), 55.4 (C^{27}), 31.7 (C^{28}, C^{32}), 31.2 (C^3, C^7), 25.3 (C^4, C^6), 24.8 (C^{29}, C^{31}), 22.9 (C^5, C^{30}), 21.6 (C^{22}), 21.5 (C^{14}). The full assignment of the signals in ^{1}H and ^{13}C NMR spectra was performed using ^{1}H−^{13}C HMBC, ^{1}H−^{13}C HSQC, NOESY, COSY NMR techniques (Figs. 9S−12S). IR (KBr, selected bands, cm^{-1}): 3168 w ν(N−H), 2934 s, 2857 w ν(C_{sp3}−H), 2235 s ν(C≡N), 1608 s ν(C = N), 1564 s ν(N−$C_{carbene}$). HRMS (ESI^+), *m*/*z*: 723.2539 $[M-Cl]^+$. $C_{32}H_{39}ClN_5Pt$ Calcd. m/z: 723.2542. Anal. Calcd. for $C_{32}H_{39}Cl_2N_5Pt\cdot CH_2Cl_2$ (844.60): C, 46.93; H, 4.89; N, 8.29. Found: C, 47.13; H, 4.93; N, 8.34.

3c: Yield 46%, red crystals. ^{1}H NMR (400 MHz, $CDCl_3$): δ 11.22 (br, 1H, N*H*), 11.13 (br, 1H, N*H*), 9.90 (br, 1H, N*H*), 7.54 (d, ^3J = 8.0 Hz, 2H, H−Ar), 7.43 (d, ^3J = 8.0 Hz, 2H, H−Ar), 7.01 (d, ^3J = 8.0 Hz, 2H, H−Ar), 6.86 (d, ^3J = 8.0 Hz, 2H, H−Ar), 4.53 (br, 1H, −*H*C(CH_2)$_5$), 3.89 (s, 3H, OCH_3), 3.86 (s, 3H, OCH_3), 3.63 (s, 1H, −*H*C(CH_2)$_5$), 2.30−1.23 (m, 20H, CH_2). ^{13}C NMR (101 MHz, $CDCl_3$): δ 184.2, 179.6, 171.0, 161.3, 161.1, 139.5, 137.0, 131.8, 131.5, 121.9, 120.4, 115.1, 114.0, 58.2, 55.2, 55.5, 55.4, 31.7, 31.2, 30.9, 25.3, 24.8, 22.8. IR (KBr, selected bands, cm^{-1}): 3433 s ν(N−H), 2924 w ν(C_{sp3}−H), 2214 s ν(C≡N), 1609 s ν(C = N), 1514 s ν(N−$C_{carbene}$). HRMS (ESI^+), *m*/*z*: 755.2419 $[M-Cl]^+$. $C_{32}H_{39}ClN_5O_2Pt$ Calcd. m/z: 755.2440. Anal. Calcd. for $C_{32}H_{39}Cl_2N_5O_2Pt$ (791.67): C, 48.55; H, 4.97; N, 8.85. Found: C, 48.18; H, 4.93; N, 8.75.

4c: Yield 45%, red crystals. ^{1}H NMR (400 MHz, $CDCl_3$): δ 11.01 (br, 1H, N*H*), 10.63 (br, 1H, NCN*H*), 9.95 (br, 1H, N*H*), 7.81 (d, ^3J = 8.0 Hz, 2H, H−Ar), 7.30 (d, ^3J = 8.0 Hz, 2H, H−Ar), 7.03 (d, ^3J = 8.0 Hz, 2H, H−Ar), 6.84 (d, ^3J = 8.0 Hz, 2H, H−Ar), 3.90 (s, 3H, OCH_3), 3.84 (s, 3H, OCH_3), 1.64 (s, 9H, *t*-Bu), 1.55 (s, 9H, *t*-Bu). IR (KBr, selected bands, cm^{-1}): 3423 s ν(N−H), 2928 w, 2831 w ν(C_{sp3}−H), 2220 m ν(C≡N), 1707 m, 1603 s ν(C = N), 1502 s ν(N−$C_{carbene}$). HRMS (ESI^+), *m*/*z*: 703.2046 $[M-Cl]^+$. $C_{28}H_{35}ClN_5O_2Pt$ Calcd. m/z: 703.2127. Anal. Calcd. for $C_{28}H_{35}Cl_2N_5O_2Pt\cdot CH_2Cl_2$ (824.53): C, 42.24; H, 4.52; N, 8.49. Found: C, 42.42; H, 4.54; N, 8.54.

5c: Yield 21%, red crystals. ^{1}H NMR (400 MHz, $CDCl_3$): δ 10.88 (br, 1H, N*H*), 9.38 (br, 1H, N*H*), 7.81−7.76 (m, 4H, H−Ar), 7.54−7.50 (m, 4H, H−Ar), 6.89−6.80 (m, 8H, H−Ar), 3.89 (s, 3H, OCH_3), 3.85 (s, 3H, OCH_3), 3.83 (s, 3H, OCH_3), 3.76 (s, 3H, OCH_3). IR (KBr, selected bands, cm^{-1}): 3443 m ν(N−H), 2932, 2835 w ν(C_{sp3}−H), 2199 m ν(C≡N) 1709 m, 1603 s ν(C = N), 1506 s ν(N−$C_{carbene}$). HRMS (ESI^+), *m*/*z*: 803.1707 $[M-Cl]^+$. $C_{34}H_{31}ClN_5O_4Pt$ Calcd. m/z: 803.1712. Anal. Calcd. for $C_{34}H_{31}Cl_2N_5O_4Pt$ (839.62): C, 48.64; H, 3.72; N, 8.34. Found: C, 48.33; H, 3.71; N, 8.27.

Synthesis of complexes **3d**−**f**: A 5 mL round-bottomed flask was equipped with a stirring bar and charged with *cis*-[$PtCl_2(CNCy)_2$] (**2a**) (0.1 mmol) and 3,4-diaryl-1*H*-pyrrol-2,5-diimine (aryl = 4-fluorophenyl (**1d**), 4-chlorophenyl (**1e**), 4-bromophenyl (**1f**)) (0.1 mmol). Anhydrous acetonitrile (4 mL) was added and the solution was stirred under reflux conditions for 5 h. Volatiles were evaporated under vacuum. The resulting solid was rinsed with acetone (1 mL) and recrystallized from the mixture of acetone and chloroform (1:2).

3d: Yield 23%, red crystals. ^{1}H NMR (400 MHz, $CDCl_3$) δ 10.86 (br, 1H, N*H*), 10.51 (br, 1H, N*H*), 10.08 (br 1H, N*H*), 7.51−7.42 (m, 4H, H−Ar), 7.05−6.95 (m, 4H, H−Ar), 4.28 (br, 1H, −*H*C(CH_2)$_5$), 4.08 (br, 1H, −*H*C(CH_2)$_5$), 2.08−1.38 (m, 20H, CH_2). IR (KBr, selected bands, cm^{-1}): 3431 m ν(N−H), 2932 m, 2854 w ν(C_{sp3}−H), 2224 s ν(C≡N), 1601 m ν(C = N), 1512 w ν(N−$C_{carbene}$). HRMS (ESI^+), *m*/*z*: 731.2037 $[M-Cl]^+$. $C_{30}H_{33}ClF_2N_5Pt$. Calcd. m/z: 731.2040.

3e: Yield 22%, orange crystals. ^{1}H NMR (400 MHz, $CDCl_3$) δ 11.84 (s, 1H, N*H*), 11.12 (s, 1H, N*H*), 9.92 (s, 1H, N*H*), 7.47 (d, ^3J = 8.8 Hz, 2H, H−Ar), 7.44 (d, ^3J = 8.8 Hz, 2H, H−Ar), 7.40 (d, ^3J = 8.8 Hz, 2H, H−Ar), 7.35 (d, ^3J = 8.8 Hz, 2H, H−Ar), 4.50−4.41 (m, 1H, −*H*C(CH_2)$_5$), 3.57 (s, 1H, −*H*C(CH_2)$_5$), 2.12−1.27 (m, 20H, CH_2). IR (KBr, selected bands, cm^{-1}): 2932 s ν(C_{sp3}−H), 2226 s ν(C≡N), 1688 m ν(C = N), 1546 s ν(N−$C_{carbene}$). HRMS (ESI^+), *m*/*z*: 763.1421 $[M-Cl]^+$. $C_{30}H_{33}Cl_3N_5Pt$. Calcd. m/z: 763.1449; 795.1683 $[M + CH_3OH]^+$. $C_{31}H_{37}Cl_3N_5OPt$. Calcd. m/z: 795.1711. Anal. Calcd. for $C_{30}H_{33}Cl_4N_5Pt\cdot CH_2Cl_2$ (885.44): C, 42.05; H, 3.98; N, 7.91. Found: C, 42.13; H, 4.01; N, 7.94.

3f: Yield 12%, orange crystals. ^{1}H NMR (400 MHz, $CDCl_3$) δ 11.93 (br, 1H, N*H*), 11.24 (br, 1H, N*H*), 9.92 (br, 1H, N*H*), 7.64 (d, ^3J = 8.4 Hz, 2H, H−Ar), 7.52 (d, ^3J = 8.4 Hz, 2H, H−Ar), 7.37 (d, ^3J = 8.4 Hz, 2H, H−Ar), 7.34 (d, ^3J = 8.4 Hz, 2H, H−Ar), 4.46 (s, 1H, −*H*C(CH_2)$_5$), 3.50 (s, 1H, −*H*C(CH_2)$_5$), 2.18−1.28 (m, 20H, CH_2). IR (KBr, selected bands, cm^{-1}): 3394 m ν(N−H), 2934 s, 2857 m ν(C_{sp3}−H), 2220 s ν(C≡N), 1572 s ν(C = N), 1542 s ν(N−$C_{carbene}$). HRMS (ESI^+), *m*/*z*: 851.0428 $[M-Cl]^+$. $C_{30}H_{33}Br_2ClN_5Pt$. Calcd. m/z: 851.0439. Anal. Calcd. for $C_{30}H_{33}Br_2Cl_2N_5Pt$ (889.40): 40.51; H, 3.74; N, 7.87. Found: 40.31; H, 3.73; N, 7.80.

4.3. General procedure for catalytic hydrosilylation of phenylacetylene

In a 5 mL round-bottomed flask equipped with a stirring bar, a solution of the selected catalyst in chloroform (2.5×10^{-4} M) was charged. The reaction flask was plugged with septum, placed into a pre-heated oil bath at 60 °C and purged with argon until complete

removal of chloroform. Further, a solution of phenylacetylene (51 mg, 0.5 mmol) and triethoxysilane (82 mg, 0.5 mmol) in anhydrous toluene (0.2 mL) was added and the reaction mixture was stirred at 100 °C. After the reaction completion, 1,2-dimethoxyethane (7.2 mg, 0.08 mmol, used as an internal standard) was added and the crude mixture was analyzed by ^{1}H NMR spectroscopy. Quantifications were performed upon integration of the selected peaks of the product against peaks of 1,2-dimethoxyethane.

4.4. Catalytic tests in polymeric systems

The cross-linking system consisted of two components: A and B.

Component A: the calculated amount of the catalyst was diluted in CH_2Cl_2 and added to PDMS, where later the mixture was stirred and dried under vacuum at RT to remove the solvent.

Component B: EHDMS and PDMS were mixed and carefully stirred.

The amounts required were calculated for the specific ratio of hydride and vinyl groups (3:1) in the reaction mixture.

To 0.5 mL of component A 0.5 mL of component B was added and stirred for 30 s. The mixture was then placed into a thermostat at 85 °C until a dry cured product was obtained. The total catalyst concentration in the resulting silicone rubber was 1.0×10^{-3}–5.0×10^{-5} mol L^{-1}.

The curing time (τ_{curing}) was measured as the time passed from mixing components A and B to the moment when cured rubber is obtained [35–37]. Curing times were measured as dry-to-touch and dry-through times according to ASTM D1640 [38], the both methods results are similar to each other. Measurements were carried out five times for each sample, duplicate determinations agreed within ±10%.

4.5. X-ray structure determination

The crystals of 3b·CH_2Cl_2 were obtained by a slow evaporation of solvent at room temperature. The crystal of compound 3b·CH_2Cl_2 was immersed in cryo-oil, mounted in a nylon loop, and analyzed at a temperature of 170 K. The X-ray diffraction data were collected on an Agilent Technologies Excalibur Eos and Supernova Atlas diffractometers. The structure has been solved by the direct methods and refined by means of the SHELXL–97 program [39] incorporated in the OLEX^2 program package [40]. The carbon-bound H atoms were placed in calculated positions and were included in the refinement in the 'riding' model approximation, with U_{iso}(H) set to1.5U_{eq}(C) and C–H 0.96 Å for CH_3 groups, U_{iso}(H) set to1.2U_{eq}(C) and C–H 0.93 Å for the CH groups, and U_{iso}(H) set to 1.2U_{eq}(N) and N–H 0.86 Å for the NH groups Empirical absorption correction was applied in CrysAlisPro program complex [41] using spherical harmonics, implemented in SCALE3 ABSPACK scaling algorithm.

The crystal structure and crystallographic details are given in Table S2. Crystal data have been deposited at the Cambridge Crystallographic Data Centre (CCDC) with deposition number CCDC 1983029 for **3b**·CH_2Cl_2.

4.6. Computational details

The full geometry optimization and total energy calculations have been carried out at the DFT hybrid level of theory using Becke's three parameter hybrid exchange functional in combination with the gradient-corrected correlation functional of Lee, Yang, and Parr (B3LYP) [42–45] and standard basis 6-31 + G(d,p) for light atoms and pseudopotential CEP 1-21G [46] for palladium using the Gaussian 03 program package [47].

4.7. Cell lines and cultivation conditions

The cytotoxicity tests were performed on three human cancer cell lines. CH1/PA-1 cells were kindly provided by Lloyd R. Kelland (CRC Centre for Cancer Therapeutics, Institute of Cancer Research, Sutton, UK). SW480 (human adenocarcinoma of the colon), A549 (human non-small cell lung cancer) were obtained from Brigitte Marian (Institute of Cancer Research, Department of Medicine I, Medical University of Vienna, Austria). Cell monolayer adherent cultures were grown in 75 cm^2 culture flasks (Starlab, Germany) in complete medium [i.e., minimal essential medium (MEM) supplemented with 10% heat-inactivated fetal bovine serum (Biowest, France), 1 mM sodium pyruvate, 1% nonessential amino acids from 100 × ready-to-use stock and 4 mM L-glutamine (all purchased from Sigma-Aldrich, Austria)]. Cell cultures were incubated at 37 °C in a moist atmosphere containing 5% CO_2.

4.8. Cytotoxicity tests in cancer cell lines

The cytotoxic activity *in vitro* was determined by means of colorimetric microculture MTT assay (MTT = 3-(4,5-dimethyl-2-thiazolyl)-2,5-diphenyl-2H-tetrazolium bromide). For this purpose, cells were harvested from culture flasks by trypsinization and seeded into 96-well plates (Starlab, Germany) in densities of 1×10^3 cells/well (CH1/PA-1), 2×10^3 cells/well (SW480) and 3×10^3 cells/well (A549) in volume of 100 μL/well. Cells were allowed to settle and resume proliferation for 24 h before exposure to the drugs. Stock solutions of each complex were prepared in DMSO, appropriately diluted in complete MEM medium (not to exceed 0.5% DMSO concentration on cells) and instantly added to the plates (100 μL/well). After continuous exposure for 96 h, drug solutions were replaced with 100 μL/well of a 1:6 MTT/RPMI 1640 solution (MTT solution, 5 mg/mL of MTT reagent in phosphate-buffered saline; RPMI 1640 medium, supplemented with 10% heat-inactivated fetal bovine serum and 4 mM L-glutamine). After incubation for 4 h, the medium/MTT mixtures were removed, and the formazan crystals formed by viable cells were dissolved in DMSO (150 μL/well). Optical densities were measured at 550 nm with a microplate reader (ELx808 Absorbance Microplate Reader, Bio-Tek, USA), using a reference wavelength of 690 nm to correct for unspecific absorption. The quantity of viable cells was expressed in relation to untreated control and 50% inhibitory concentrations (IC50) were calculated from concentration-effect curves by interpolation. Evaluation is based on means from at least three independent experiments, each comprising triplicate per concentration level.

Declaration of competing interest

The authors declare that they have no known competing financial interests or personal relationships that could have appeared to influence the work reported in this paper.

Acknowledgments

A part concerning to synthesis, photophysical properties, and catalytic activity of the ADC-platinum(II) complexes was supported by the Government of Saint Petersburg (grant N 4ntd-19 from November 15, 2019, T.G.C.). A part on photophysical properties of silicone rubbers was supported by the Russian Science Foundation (project 20-19-00256, R.M.I.). The authors are grateful to Academician V. Yu. Kukushkin (Saint Petersburg State University) for fruitful discussions. The authors also thank the Centre for Optical and Laser Materials Research, Centre for Chemical Analysis and Materials Research, Cryogenic Department, and Centre of Magnetic

Resonance (all belong to Saint Petersburg State University) for physicochemical measurements.

Appendix A. Supplementary data

Supplementary data to this article can be found online at https://doi.org/10.1016/j.jorganchem.2020.121435.

References

[1] L.M. Slaughter, Acyclic aminocarbenes in catalysis, ACS Catal. 2 (2012) 1802–1816, https://doi.org/10.1021/cs300300y.

[2] V.P. Boyarskiy, K.V. Luzyanin, V.Y. Kukushkin, Acyclic diaminocarbenes (ADCs) as a promising alternative to N-heterocyclic carbenes (NHCs) in transition metal catalyzed organic transformations, Coord. Chem. Rev. 256 (2012) 2029–2056, https://doi.org/10.1016/j.ccr.2012.04.022.

[3] H.V. Huynh, The Organometallic Chemistry of N-Heterocyclic Carbenes, John Wiley & Sons, Inc., Chichester, UK, 2017.

[4] H.V. Huynh, Electronic properties of N-heterocyclic carbenes and their experimental determination, Chem. Rev. 118 (2018) 9457–9492, https://doi.org/10.1021/acs.chemrev.8b00067.

[5] S.P. Nolan (Ed.), N-heterocyclic Carbenes: Effective Tools for Organometallic Synthesis, Wiley-VCH, Weinheim, 2014.

[6] R.W. Alder, P.R. Allen, M. Murray, A.G. Orpen, Bis(diisopropylamino)carbene, Angew Chem. Int. Ed. Engl. 5 (1996) 1121–1123, https://doi.org/10.1002/anie.199611211.

[7] E.L. Rosen, M.D. Sanderson, S. Saravanakumar, C.W. Bielawski, Synthesis and study of the first N-aryl acyclic diaminocarbene and its transition-metal complexes, Organometallics 26 (2007) 5774–5777, https://doi.org/10.1021/om7007925.

[8] M.S. Collins, E.L. Rosen, V.M. Lynch, C.W. Bielawski, Differentially substituted acyclic diaminocarbene ligands display conformation-dependent donicities, Organometallics 29 (2010) 3047–3053, https://doi.org/10.1021/om1004226.

[9] R.A. Michelin, A.J.L. Pombeiro, M.F.C. Guedes da Silva, Aminocarbene complexes derived from nucleophilic addition to isocyanide ligands, Coord. Chem. Rev. 218 (2001) 75–112.

[10] K.V. Luzyanin, A.J.L. Pombeiro, in: V. Nenajdenko (Ed.), Carbene Complexes Derived Form Metal-Bound Isocyanides, Wiley-VCH, 2012, pp. 531–550.

[11] V.P. Boyarskiy, N.A. Bokach, K.V. Luzyanin, V.Y. Kukushkin, Metal-mediated and metal-catalyzed reactions of isocyanides, Chem. Rev. 115 (2015) 2698–2779, https://doi.org/10.1021/cr500380d.

[12] M.A. Kinzhalov, K.V. Luzyanin, V.P. Boyarskiy, M. Haukka, V.Y. Kukushkin, ADC-based palladium catalysts for aqueous suzuki-miyaura cross-coupling exhibit greater activity than the most advantageous catalytic systems, Organometallics 32 (2013) 5212–5223, https://doi.org/10.1021/om4007592.

[13] K.V. Luzyanin, A.G. Tskhovrebov, M. Carolina Carias, M. Fátima C Guedes Da Silva, A.J.L. Pombeiro, V.Y. Kukushkin, Novel Metal-mediated (M = Pd, Pt) coupling between isonitriles and benzophenone hydrazone as a route to aminocarbene complexes exhibiting high catalytic activity (M = Pd) in the Suzuki-Miyaura reaction, Organometallics 28 (2009) 6559–6566, https://doi.org/10.1021/om900682v.

[14] R.S. Chay, K.V. Luzyanin, Evaluation of catalytic properties of aminocarbene species derived from the integration between 3-iminoisoindolin-1-ones and palladium-bound isonitriles in Suzuki-Miyaura cross-coupling, Inorg. Chim. Acta. 380 (2012) 322–327, https://doi.org/10.1016/j.ica.2011.09.047.

[15] R.S. Chay, K.V. Luzyanin, V.Y. Kukushkin, M.F.C. Guedes Da Silva, A.J.L. Pombeiro, Novel palladium-aminocarbene species derived from metal-mediated coupling of isonitriles and 1,3-diiminoisoindoline: synthesis and catalytic application in Suzuki-Miyaura cross-coupling, Organometallics 31 (2012) 2379–2387, https://doi.org/10.1021/om300020j.

[16] B.G.M. Rocha, E.A. Valishina, R.S. Chay, M.F.C. Guedes Da Silva, T.M. Buslaeva, A.J.L. Pombeiro, V.Y. Kukushkin, K.V. Luzyanin, ADC-metal complexes as effective catalysts for hydrosilylation of alkynes, J. Catal. 309 (2014) 79–86, https://doi.org/10.1016/j.jcat.2013.09.003.

[17] R.S. Chay, B.G.M. Rocha, A.J.L. Pombeiro, V.Y. Kukushkin, K.V. Luzyanin, Platinum complexes with chelating acyclic aminocarbene ligands work as catalysts for hydrosilylation of alkynes, ACS Omega 3 (2017) 863–871, https://doi.org/10.1021/acsomega.7b01688.

[18] D.V. Boyarskaya, E. Bulatov, I.A. Boyarskaya, T.G. Chulkova, V.A. Rassadin, E.G. Tolstopjatova, I.E. Kolesnikov, M.S. Avdontceva, T.L. Panikorovskii, V.V. Suslonov, M. Haukka, Syntheses and structures of a series of acyclic diaminocarbene palladium(II) complexes derived from 3,4-diaryl-1*H*-pyrrol-2,5-diimines and bisisocyanide palladium(II) complexes, Organometallics 38 (2019) 300–309, https://doi.org/10.1021/acs.organomet.8b00725.

[19] K.V. Luzyanin, A.J.L. Pombeiro, M. Haukka, V.Y. Kukushkin, Coupling between 3-Iminoisoindolin-1-ones and complexed isonitriles as a metal-mediated route to a novel type of palladium and platinum iminocarbene species, Organometallics 27 (2008) 5379–5389, https://doi.org/10.1021/om800517c.

[20] A.M. Afanasenko, D.V. Boyarskaya, I.A. Boyarskaya, T.G. Chulkova, Y.M. Grigoriev, I.E. Kolesnikov, M.S. Avdontceva, T.L. Panikorovskii, A.I. Panin, A.N. Vereshchagin, M.N. Elinson, Structures and photophysical properties of 3,4-diaryl-1H-pyrrol-2,5-diimines and 2,3-diarylmaleimides, J. Mol. Struct. 1146 (2017) 554–561, https://doi.org/10.1016/j.molstruc.2017.06.048.

[21] L. Mercs, M. Albrecht, Beyond catalysis: N-heterocyclic carbene complexes as components for medicinal, luminescent, and functional materials applications, Chem. Soc. Rev. 39 (2010) 1903–1912, https://doi.org/10.1039/b902238b.

[22] R. Jazzar, M. Soleilhavoup, G. Bertrand, Cyclic (alkyl)- and (Aryl)-(amino)carbene coinage metal complexes and their applications, Chem. Rev. 120 (2020) 4141–4168, https://doi.org/10.1021/acs.chemrev.0c00043.

[23] T.V. Serebryanskaya, M.A. Kinzhalov, V. Bakulev, G. Alekseev, A. Andreeva, P.V. Gushchin, A.V. Protas, A.S. Smirnov, T.L. Panikorovskii, P. Lippmann, I. Ott, C.M. Verbilo, A.V. Zuraev, A.S. Bunev, V.P. Boyarskiy, N.A. Kasyanenko, Water soluble palladium(ii) and platinum(ii) acyclic diaminocarbene complexes: solution behavior, DNA binding, and antiproliferative activity, New J. Chem. 44 (2020) 5762–5773, https://doi.org/10.1039/d0nj00060d.

[24] B. Bertrand, A.S. Romanov, M. Brooks, J. Davis, C. Schmidt, I. Ott, M. O'Connell, M. Bochmann, Synthesis, structure and cytotoxicity of cyclic (alkyl)(amino) carbene and acyclic carbene complexes of group 11 metals, Dalton Trans. 46 (2017) 15875–15887, https://doi.org/10.1039/c7dt03189k.

[25] S. Montanel-Pérez, R. Elizalde, A. Laguna, M.D. Villacampa, M.C. Gimeno, Synthesis of bioactive N-acyclic gold(I) and gold(III) diamino carbenes with different ancillary ligands, Eur. J. Inorg. Chem. 2019 (2019) 4273–4281, https://doi.org/10.1002/ejic.201900606.

[26] Y.Y. Scaffidi-Domianello, A.A. Legin, M.A. Jakupec, A. Roller, V.Y. Kukushkin, M. Galanski, B.K. Keppler, Novel oximato-bridged platinum(II) di- and trimer(s): synthetic, structural, and in vitro anticancer activity studies, Inorg. Chem. 51 (2012) 7153–7163, https://doi.org/10.1021/ic300148e.

[27] M. Poyatos, A. Maisse-François, S. Bellemin-Laponnaz, L.H. Gade, Coordination chemistry of a modular N,C-chelating oxazole-carbene ligand and its applications in hydrosilylation catalysis, Organometallics 25 (2006) 2634–2641, https://doi.org/10.1021/om060166u.

[28] J.J. Hu, F. Li, T.S. Andy Hor, Novel Pt(II) mono- and biscarbene complexes: synthesis, structural characterization and application in hydrosilylation catalysis jian, Organometallics 28 (2009) 1212–1220, https://doi.org/10.1016/j.jorganchem.2008.10.048.

[29] G.F. Silbestri, J.C. Flores, E. De Jesús, Water-soluble N-heterocyclic carbene platinum(0) complexes: recyclable catalysts for the hydrosilylation of alkynes in water at room temperature, Organometallics 31 (2012) 3355–3360, https://doi.org/10.1021/om300148q.

[30] C. Lu, S. Gu, W. Chen, H. Qiu, Platinum(ii) complexes with polydentate N-heterocyclic carbenes: synthesis, structural characterization and hydrosilylation catalysis, Dalton Trans. 39 (2010) 4198–4204, https://doi.org/10.1039/b924587a.

[31] A. Cook, R. Linstead, Phthalocyanines. Part XI . The preparation of octaphenylporphyrazines from diphenylmaleinitrile, J. Chem. Soc. (1937) 929–933, https://doi.org/10.1039/JR9370000929.

[32] T.F. Baumann, A.G.M. Barrett, B.M. Hoffman, Porphyrazine binaries: synthesis, characterization, and spectroscopy of a metal-linked trinuclear porphyrazine dimer, Inorg. Chem. 36 (1997) 5661–5665, https://doi.org/10.1021/ic9701367.

[33] F. Bonati, G. Minghetti, New isocyanide complexes of platinum(II), J. Organomet. Chem. 24 (1970) 251–256, https://doi.org/10.1016/S0022-328X(00)91586-9.

[34] A.G. Tskhovrebov, K.V. Luzyanin, M. Haukka, V.Y. Kukushkin, Synthesis and characterization of cis-(RNC)2PtII species useful as synthons for generation of various (aminocarbene)Pt II complexes, J. Chem. Crystallogr. 42 (2012) 1170–1175, https://doi.org/10.1007/s10870-012-0371-0.

[35] M.J. Owen, The Polysiloxanes, Silicon 8 (2016) 617–618, https://doi.org/10.1007/s12633-015-9306-7.

[36] J. Li, J. Peng, Y. Deng, C. Ma, G. Zhang, Y. Bai, G. Lai, Synthesis of platinum acetylide complexes and their application in curing silicone rubber by hydrosilylation, Appl. Organomet. Chem. 26 (2012) 461–466, https://doi.org/10.1002/aoc.2881.

[37] I. Kownacki, B. Marciniec, K. Szubert, M. Kubicki, M. Jankowska, H. Steinberger, S. Rubinsztajn, Tris(triorganosilyl)phosphites-New ligands controlling catalytic activity of Pt(0) complex in curing of silicone rubber, Appl. Catal. Gen. 380 (2010) 105–112, https://doi.org/10.1016/j.apcata.2010.03.041.

[38] J. Koleske (Ed.), Paint and Coating Testing Manual: 15th. Ed of the Gardner-Sward Handbook, 15th. ed., ASTM International, West Conshohocken, PA, 2012.

[39] G.M. Sheldrick, A short history of SHELX, Acta Crystallogr. A. 64 (2008) 112–122, https://doi.org/10.1107/S0108767307043930.

[40] O.V. Dolomanov, L.J. Bourhis, R.J. Gildea, J.A.K. Howard, H. Puschmann, OLEX2 : a complete structure solution, refinement and analysis program, J. Appl. Crystallogr. 42 (2009) 339–341, https://doi.org/10.1107/s0021889808042726.

[41] CrysAlisPro, Agilent Technologies, Version 1.171.36.20 (Release 27 06 2012).

[42] A.D. Becke, Density-functional thermochemistry. III. The role of exact exchange, J. Chem. Phys. 98 (1993) 5648–5652, https://doi.org/10.1063/1.464913.

[43] P.J. Stephens, F.J. Devlin, C.S. Ashvar, C.F. Chabalowski, M.J. Frisch, Theoretical calculation of vibrational circular dichroism spectra, Faraday Discuss 99 (1994) 103–119, https://doi.org/10.1039/FD9949900103.

[44] P.J. Stephens, F.J. Devlin, C.F. Chabalowski, M.J. Frisch, Ab Initio calculation of vibrational absorption and circular dichroism spectra using density functional

force fields, J. Phys. Chem. 98 (1994) 11623–11627, https://doi.org/10.1021/j100096a001.
[45] C. Lee, W. Yang, R.G. Parr, Development of the Colle-Salvetti correlation-energy formula into a functional of the electron density, Phys. Rev. B 37 (1988) 785–789, https://doi.org/10.1103/PhysRevB.37.785.
[46] W.J. Stevens, M. Krauss, H. Basch, P.G. Jasien, Relativistic compact effective potentials and efficient shared-exponent basis-sets for the 3rd-row, 4th-row and 5th-row atoms, Can. J. Chem. 70 (1992) 612–630, https://doi.org/10.1139/v92-085.
[47] P.J.A. Frisch, M.J. Trucks, G.W. Schlegel, H.B. Scuseria, G.E. Robb, M.A. Cheeseman, J.R. Montgomery, J.A. Vreven Jr, T. Kudin, K.N. Burant, J.C. Millam, J.M. Iyengar, S.S. Tomasi, J. Barone, V. Mennucci, B. Cossi, M. Scalmani, G. Rega, N. Petersson, Gaussian 03, (2003).